Geometry Optimization of Metal Complexes Using Natural Internal Coordinates: Representation of Skeletal Degrees of Freedom

ATTILA BÉRCES

The Steacie Institute for Molecular Sciences, National Research Council, 100 Sussex Drive, Ottawa, Ontario K1A 0R6, Canada

Received 16 November 1995; accepted 19 March 1996

ABSTRACT

The geometry optimization using natural internal coordinates was applied for transition metal complexes. The original definitions were extended here for the skeletal degrees of freedom which are related to the translational and rotational displacements of the η^n-bonded ligands. We suggest definitions for skeletal coordinates of η^n-bonded small unsaturated rings and chains. The performance of geometry optimizations using the suggested coordinates were tested on various conformers of 14 complexes. Consideration was given to alternative representations of the skeletal internal coordinates, and the performance of optimization is compared. Using the skeletal internal coordinates presented here, most transition metal complexes were optimized between 10 and 20 geometry optimization cycles in spite of the usually poor starting geometry and crude approximation for the Hessian. We also optimized the geometry of some complexes in Cartesian coordinates using the Hessian from a parametrized redundant force field. We found that it took between two and three times as many iterations to reach convergence in Cartesian coordinates than using natural internal coordinates.

Introduction

One of the most frequently calculated molecular properties performed by quantum mechanical methods is geometry. The cost of these calculations greatly depends on the efficiency of the optimization algorithm and the choice of optimization variables. Recently, in this area of research the emphasis has been shifted toward finding the most suitable optimization variables.[1,2] Forgarasi et al. and Pulay and coworkers showed that appropriately chosen internal coordinates can be ideal optimization variables.[1,3] These *natural*

E-mail: attila@ned1.sims.nrc.ca

CCC 0192-8651 / 97 / 010045-11

internal coordinates reduce both harmonic and anharmonic coupling between coordinates to a minimum based purely on the topology of the molecules. The small harmonic coupling ensures that the method is successful even with a highly approximate Hessian. The small anharmonic coupling plays a significant role when the starting structure is poor and large displacements are required to reach the energy minimum. These qualities make the natural internal coordinate optimization especially appropriate for the location of equilibrium geometries for transition metal complexes. For these systems, neither the starting geometry nor the Hessian can be estimated fairly accurately the way it could be done for organic molecules based on molecular mechanics methods. However, for the application of natural internal coordinates for metal complexes one has to consider the representation of certain characteristic internal displacements of coordination compounds.

The internal coordinates of coordination compounds with η^n-bonds fall into two categories: ligand coordinates and skeletal coordinates. The skeletal movements represent the displacement of an entire ligand with respect to the central atom. Some examples of these internal motions are ligand–metal stretching, ligand tilt, and ligand internal rotation, skeletal bending, or skeletal torsion of the molecule. The ligand coordinates, the regular bond stretches and deformations, are suitably represented by the recommendation of Forgarasi et al.[1] However, the natural internal coordinate representation of skeletal internal movements was previously not considered until very recently. We studied the force fields of ferrocene, dibenzene-chromium, and benzene-chromium-tricarbonyl, and compared the force constants to that of the free Cp and benzene rings.[4] This comparison required a physically meaningful definition of the skeletal internal movements. We studied a few different possibilities and found that the most suitable representation involves internal coordinates expressed with the help of the centroid of the η^n-bonded ligands. These coordinates provided small coupling force constants between the skeletal and other coordinates. Usually the internal coordinate system that is appropriate for the normal coordinate analysis, also performs well in geometry optimization. Here we discuss the implementation of these internal coordinates in geometry optimization and address the problem of optimization of metal complexes in general. Figure 1 shows the structures of metal complexes considered in the present study.

Computational Details

The reported calculations were carried out using the Amsterdam density functional (ADF) program system developed by Baerends and colleagues[5a] and vectorized by Ravenek.[5b] Boerrigter et al.[6] developed the numerical integration procedure. All optimized geometries in this study were calculated based on the local density approximation (LDA).[7a] Here, we are concerned with the performance of geometry optimization, rather than the performance of the density functional calculations in terms that reproduce experimental results. To obtain better agreement with experiment, gradient corrections to the exchange[7b] and correlation[7c] potentials should have been included in the Hamiltonian. The geometries were optimized based on the GDIIS technique[8] using natural internal coordinates. We interfaced the ADF program with the GDIIS program[4,9] and implemented the skeletal coordinates discussed here.

Physical Nature of Skeletal Degrees of Freedom

From a topological point of view, there are two types of bonds between metals and organic molecules. If the metal is connected to only one carbon atom of a ligand, a monohapto bond is formed that is topologically very similar to the bonds of regular organic molecules. Accordingly, the definition of internal coordinates is also similar to that of organic molecules. On the other hand, the metal atom can bind to an organic ligand through several carbon atoms, forming a multicenter η^n-bond. The most well-known examples of this bonding situation are the sandwich-type transition metal complexes such as ferrocene and dibenzene-chromium. There are unique internal motions associated with the η^n-bonds that are different from those of regular bonds. Consequently, to describe these internal motions, one has to use unusual internal coordinate representations. In η^n-bonded metal complexes the new types of internal motions are the movement of a rigid fragment with respect to the central atom, which we refer to as skeletal degrees of freedom. For example, the C_5H_5 ring of ferrocene can move away from the metal, representing a metal–ligand

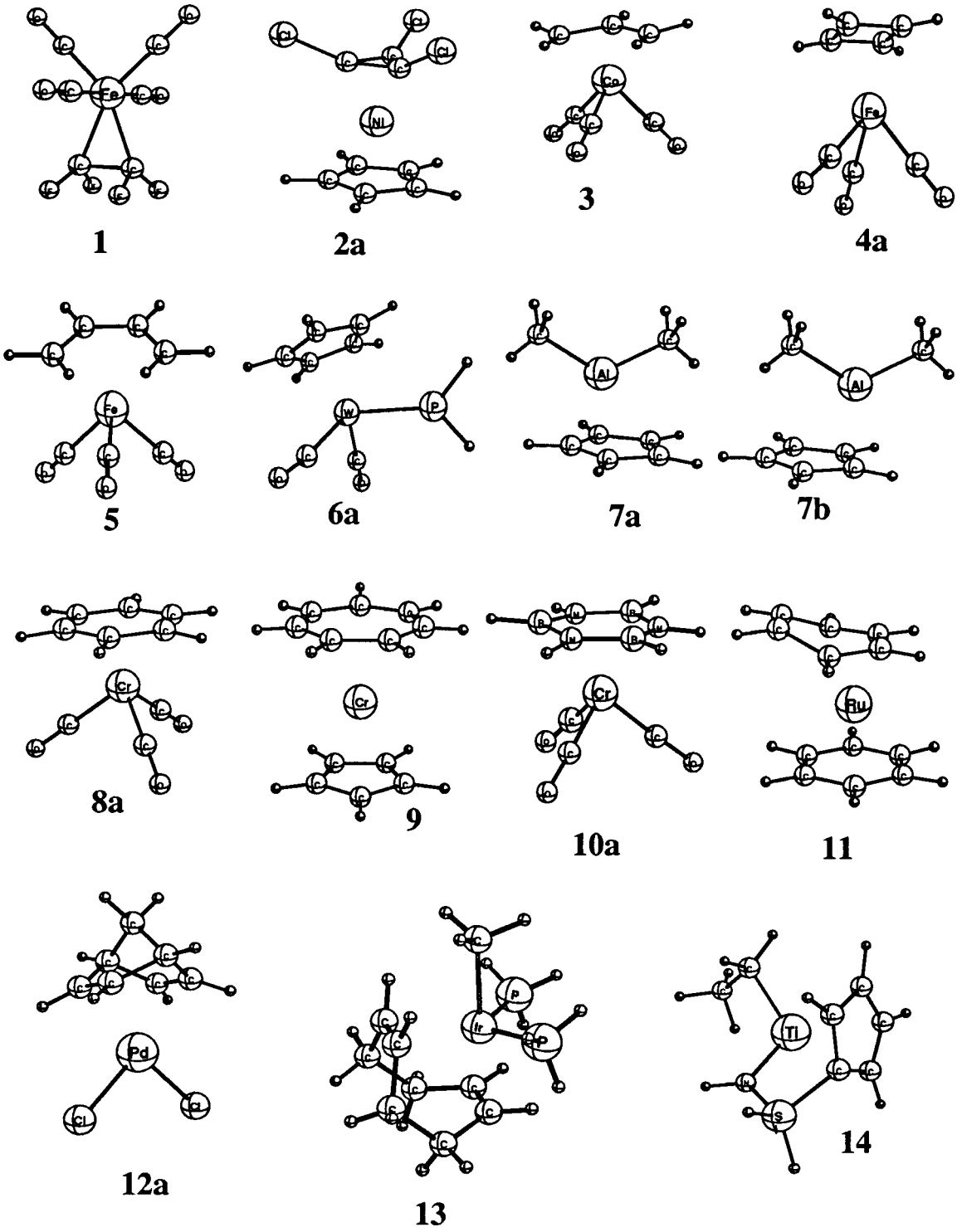

FIGURE 1. Structures of metal complexes.

stretching, or the ring can tilt or rotate around the molecular C_5 axis.

Any nonlinear molecule composed of two nonlinear fragments possesses six more internal degrees of freedom compared to the internal degrees of freedom of its two fragments. The six new internal degrees of freedom and the skeletal degrees of freedom of metal complexes in particular are related to the translational and rotational displacements of the separate fragments. Accord-

ingly, a sensible approach to find the best representation of the skeletal degrees of freedom of a complex is to regard them as an assembly of two fragments. As an example, we consider benzene-chromium-tricarbonyl as an assembly of benzene and chromium-tricarbonyl. In Figure 2 we compare the number of vibrational (or internal), transitional, and rotational degrees of freedom between the fragments and the complex.

All skeletal movements can be characterized as either a translational or a rotational motion of the ligand. Because translations and rotations of the fragments are relative to each other, we consider the movements of the benzene ring (or the ligand in general) with respect to the rest of the complex. For the skeletal internal motions resulting from the translational motion, the benzene ring can be regarded as a point mass. To find the new degrees of freedom related to translation of the ligand, one can consider a molecule in which the ligand ring is replaced by an ordinary atom. Figure 3a, b shows such situations; Figure 3a represents the metal–ligand stretch. Figure 3b shows one of the two degenerate ligand–metal–carbon bending coordinates.

The rest of the skeletal movements can be related to the rotational motion of the free fragments. The rotation of the benzene ring around the molecular symmetry axis results in an internal rotation (Fig. 4a). The rotation of the benzene ring around an axis in the plane of benzene results in a ring; one of the two degenerate tilting coordinates is shown in Fig. 4b.

In the example of $BzCr(CO)_3$, the six new degrees of freedom, compared to the separate fragments, can be accounted for as one metal–ligand stretch, two ligand–metal–carbon deformations, one internal rotation, and two ligand tilts. This argument can be generalized to any complex, and

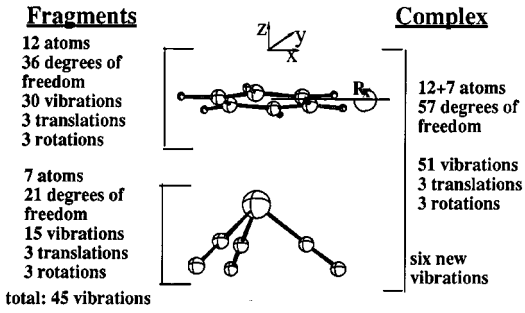

FIGURE 2. Internal and external degrees of freedom of benzene-chromium-tricarbonyl.

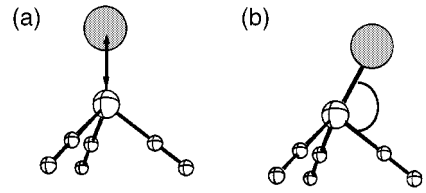

FIGURE 3. (a) Metal–ligand stretching. (b) Ligand–metal–carbon bending.

it can be shown that the skeletal movements resulting from one ligand bonded in a multicentral fashion consists of three translational type and three rotational type movements. This problem is similar to finding the lattice vibrations of a single crystal, consisting of more than one molecule per unit cell. Further, similar to the vibrations in a single crystal, the complete symmetry (or local symmetry) analysis of all internal coordinates including the skeletal ones can be made by the method of factor group analysis developed by Bhagavantam and Venkatarayudu.[10]

The representation of the translational-type skeletal vibrations is fairly straightforward by introducing the centroid to represent the movement of the entire ligand and defining bond length and angles with the help of the centroid. Rotational-type movements can also be handled similarly, however, they require further considerations. Note that rotation-type internal movements are not unique to transition metal complexes. The simplest example is the internal rotation of ethane. However, in the case of the internal rotation of the CH_3 group in organic molecules, the axis of rotation coincides with the CC bond. Therefore, this rotation can be appropriately represented by dihedral angles around the CC bond. The rotational movements of a ligand in a metal complex can be represented by bond angles and dihedral angles that involve the centroid, because the rotation is usually around the centroid-metal or centroid-carbon vectors.

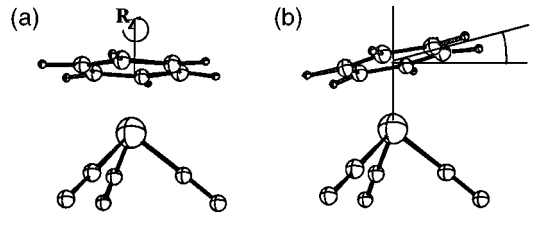

FIGURE 4. (a) Internal rotation. (b) Ligand tilt.

An example of the bending angles representing the ring tilt is shown on Figure 5a. Six such bending angles, $\alpha_{d1}, \alpha_{d2}, \ldots, \alpha_{d6}$ can be defined for $BzCr(CO)_3$. Appropriately chosen linear combinations of these six such bending angles can represent the two orthogonal tilting motions of the ring. The internal rotation can be represented as a dihedral angle involving a ring carbon atom, the reference point, the metal atom, and another carbon from the CO group, as shown on Figure 5b. Altogether 18 such dihedral angles can be defined for $BzCr(CO)_3$, and the internal rotation can be expressed with an equally weighted linear combination of all 18 of these dihedral angles.

In the *Z*-matrix optimization method it is also possible to introduce dummy atoms to facilitate the definition of such bending and torsion angles as shown in **4a** and **4b**. However, if one introduces a dummy atom in the scheme of the *Z*-matrix optimization, it increases the number of degrees of freedom. Therefore, *Z*-matrix dummy atoms are not appropriate for the present purpose. For this reason, we avoided the use of the words dummy atom for the explanation of these internal coordinates. The introduction of such a reference point that does not increase the number of degrees of freedom was first addressed by Doman et al. in connection with molecular mechanics type optimization of metallocenes.[11] These authors suggested the elimination of the forces on the dummy atom by distributing them to real atoms. Kaupp and Schleyer also used the centroid approach to determine the energy profile of bent metallocenes as a function of the skeletal bending angle.[12] However, previously the definition of internal coordinates with the centroid was applied to only special cases and not generalized for gradient based geometry optimization.

For the transformation of forces between internal and Cartesian coordinates, one needs the derivatives of the internal coordinates as a function of Cartesian coordinates. Such differentiation involving dummy atoms or a reference point has to be done by applying the chain rule,

$$\frac{dq_i\left(x_k, \ldots, x_j, \ldots, x_R(x_m, \ldots, x_n), \ldots, x_l\right)}{dx_j} = \frac{\partial q_i}{\partial x_j} + \frac{\partial q_i}{\partial x_R}\frac{\partial x_R}{\partial x_j}. \quad (1)$$

Atoms $j = k, \ldots, l$ define the internal coordinate, while atoms $j = m, \ldots, n$ define the reference point x_R. The position x_R is defined in the form of a function of the coordinates of the defining atoms. The two most obvious choices for x_R are the center of mass and the geometrical central of the bonded atoms. The center of mass is expressed as

$$x_R(x_m, \ldots, x_n) = \frac{1}{M}\sum_{i=m}^{n} m_i x_i \quad (2)$$

where m_i and M are the atomic and fragment masses, respectively. The geometrical center is defined as

$$x_R(x_m, \ldots, x_n) = \frac{1}{n-m+1}\sum_{i=m}^{n} x_i. \quad (3)$$

We previously compared the consequences of defining the reference point by eqs. (2) and (3) in connection with the normal coordinate analysis of ferrocene.[4] The center of mass as a reference point introduces mass dependence of the internal coordinates. Therefore, the internal coordinate definitions of different isotopomers of the same compound are also different, resulting in a different set of force constants for different isotopomers. These differences between force constants of isotopomers are the artifacts of the mass dependent reference point definitions.

When eq. (3) is used to define the reference point one has to specify which atoms of the fragments should be included in the definition. In our example of $BzCr(CO)_3$, we introduced the geometrical center of the carbon atoms of the benzene ring. If we had included the hydrogen atoms as well, the reference point would coincide with the geometrical center of the carbon atoms for a planar ring but it would lead to a different definition of skeletal coordinates. The most physically meaningful reference point is the geometrical center of the atoms bonded to the metal atom. For example, if a six membered ring is bound in an η^4-bonded fashion, than only the four bonded carbons should define the reference point. Further examples are given in the next section.

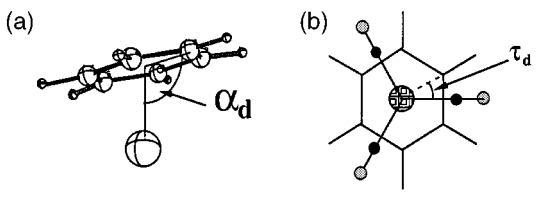

FIGURE 5. (a) Bending angle defined by a reference point. (b) Dihedral angle defined with a reference point.

Skeletal Internal Coordinates for η^n-Bonded Ligands

In this section we apply the principles described above to select the skeletal internal coordinates of some transition metal complexes with small aromatic rings and unsaturated chains as ligands. Here we deal with only the skeletal coordinates; the rest of the coordinates can be defined by the standard procedures.[1] As discussed in the previous section, one has to define four types of skeletal internal coordinates: stretchings, bendings, internal rotations, and ligand tiltings. The definition of the ligand tilting coordinates can be expressed with a general formula; the rest of the skeletal coordinate definitions depend on the actual structure.

The tilting coordinates are represented by a pair of linear combinations of C–*D*–M angles α_D, where C is a ring atom (usually carbon), *D* is the reference point, and M is the central metal (see Fig. 5a). The linear combination coefficients can be derived from group theory, considering C_{nv} local symmetry for the *n*-membered η^n-bonded ligands.

$$q^a = \sum_{k=1}^{n} \cos\{(k-1)2\pi/n\}\alpha_{D_k}, \qquad (4)$$

$$q^b = \sum_{k=1}^{n} \sin\{(k-1)2\pi/n\}\alpha_{D_k}. \qquad (5)$$

EXAMPLES

Figure 1 shows several examples of transition metal complexes with ligands ranging from C_2F_4 to an eight membered ring. We included the internal coordinates of selected complexes in Table I.

The simplest unsaturated ligand is the C_2F_4 represented in the Fe complex **1**. In this particular simple case, physically meaningful definition can also be accomplished by regular stretching, bending, and torsional coordinates or equivalently by the principles outlined above.

The example of a three and a five membered aromatic ring is represented by $Ni(C_3Cl_3)(C_5H_5)$

TABLE I.
Definition of Skeletal Internal Coordinates

Lig. Type	Struct. No.	Internal Coordinate	Description
η^3-3-ring	**2a**	Ni–*D* distance, where *D* is the centroid	Skeletal stretch
		$q = 2\alpha_{D2} - \alpha_{D1} - \alpha_{D3}$, where α_{Di} is shown in Fig. **4b**	Tilt a
		$q = \alpha_{D1} - \alpha_{D3}$	Tilt b
		$q = \sum_{i,ji}^{j} \tau_D$, where ${}_i^j\tau_D$ is a dihedral angle between C_i atoms of the ligand, the centroid (*D*), the central metal atom and the bonded atoms of other ligands X_j ($i = 1, 2, 3$, and $j = 1, \ldots, 5$ in this case); see Fig. **4a**	Internal rotation
		A pair of perpendicular bending angles between D_1–Ni–D_2, where D_1 and D_2 are the centroids of the upper and lower ring, respectively	Skeletal bend
η^3-3-chain	**3**	Same as above	Skeletal stretch
		Same as for η^3-3-ring	Tilt a and b
		Same as for η^3-3-ring, except X_j atoms are the three carbon atoms of the CO ligands, $j = 1, 2, 3$	Internal rotation
		$q = \beta_{D1} - \beta_{D3}$ where β_{D1} is defined as the angle between *D*–Co–C_j, $j = 1, 2, 3$ the carbon atoms of the CO ligands	Skeletal bending
		$q = 2\beta_{D2} - \beta_{D1} - \beta_{D3}$	Skeletal bending
η^3-5-ring	**7a**	The centroid is placed in the geometrical center of the three bonded carbon atoms	Remark
		Centroid, Al distance	Stretch
		Same as for three membered ring **2a** or **3**	Tilt a–b
		This involves three carbon atoms of the ring, $i = 1, 2, 3$, as well as the two methyl C atoms, $j = 1, 2$	Internal rotation
		The displacement of *D*, out of the plane defined by Al and the two methyl carbons	Sk. out of plane deformation
		$q = \gamma - \beta_{D1} - \beta_{D2}$, where γ is the C_1–Al–C_2 angle, C are the methyl carbons	Sk. bend a

complex in structure **2a**. The corresponding coordinates for the three membered ring are included in Table I. Structure **3** shows an allyl complex, $Co(C_3H_5)(CO)_3$, which is an example for a complex with a three membered open chain. The tilting coordinates can be defined the same way for the open chain as for the ring.

The cyclobutadiene-iron-tricarbonyl complex shown in structure **4a** represents an example for a four membered ring ligand. For the tilting coordinates of the two combinations obtained from eqs. (4) and (5), one obtains $1, 0, -1, 0$ and $0, 1, 0, -1$. These combinations, however, are not the most ideal for all conformations. For example, in a conformation with the symmetry plane intersecting bonds, rather than atoms, the $1, 1, -1, -1$ and $1, -1, -1, 1$ combinations are more appropriate. The complex in structure **5** represents the open chain analogue of structure **4a**. The skeletal coordinates of structures **4** and **5** are almost identical.

The complexes in structures **6a**, **7a**, and **7b** represent the cyclopentadienyl complexes with η^5, η^3, and η^2 coordination modes. Although all of these complexes involve the same ligand, the definition of skeletal internal coordinates is different in each case. The skeletal internal coordinates are determined by the coordination mode, rather than by the ligand itself. For the η^5 coordinated ring, the C_{5v} local symmetry was used to select the tilting and internal rotation coordinates; for the η^3 complex it is more appropriate to consider the threefold local symmetry. Further, the η^2 coordinated complex (structure **7b**) is similar to the example of the C_2F_4 complex in structure **1**. For this complex it is possible to define the internal coordinates without considering the centroid.

Examples of six membered rings are shown in structures **8a**, **10a**, **11**, and **12a**. Molecules in structures **8** and **10** are analogous; the only difference is that the benzene ring was changed to its inorganic analogue borazine. Both complexes are η^6 bonded, and the internal coordinate sets are identical. In dibenzene-ruthenium (structure **11**) there is one η^6 and one η^4 bonded benzene ring. The definitions for the η^6 bonded ring are similar to that of the other benzene complexes. However, the skeletal movements of the η^4 bonded benzene are defined analogous to those of the butadiene complexes. The six membered ring of structure **12a** is coordinated with two η^2 bonds. However, for the definition of the skeletal coordinates it can be regarded as a complex with one η^4 coordination. Accordingly, the skeletal internal coordinates are analogous to those of the cyclobutadiene complex.

For the sake of completeness, we included a complex with a seven membered η^7 coordinated ring in structure **9**. This example represents the largest number of equivalently bound carbon atoms in one ligand. The (cycloocta-1,5-diene)diphosphino-methyliridium complex shown in structure **13** represents the largest ligand and is also an example for a single ligand occupying two different (an equatorial and an axial) coordination sites. The Ir complex in structure **13** could be considered as an η^4 coordinated or two η^2 coordinated ligands. Because this ligand occupies two different coordination sites, we prefer to regard the molecule as two η^2 coordinated. Clearly the two metal ligand bonds are not equivalent. Therefore, it is more appropriate to represent them by two different centroid-metal bonds. We used trigonal bipiramidal local symmetry around the central atom.

The complex shown in structure **14** represents an example where the centroid of the η^5 bonded fragment is part of another five membered ring.

Performance of Geometry Optimization

The significance of the skeletal internal coordinate definitions can be shown by their application as optimization variables in the geometry optimization of metal complexes. We optimized the geometry of the complexes described in the previous two sections and the performance of this procedure is discussed here. In addition, we compared the performance of the optimization with another alternative definition of skeletal coordinates. Most skeletal internal coordinates could also be expressed without introducing the reference point. These alternatives are considered in this section. Further, we compared the performance between optimization using Cartesian versus natural internal coordinates.

In Table II we summarize the initial and final gradients, the number of optimization steps, and the largest internal coordinate changes in the last step for each complex optimized in this study. Generally all optimizations converged in 10–20 steps, depending on the symmetry, size, quality of the initial geometry, and the Hessian. As convergence criterion, we considered the geometry converged if the maximum gradient was below 0.001 mdyn, the maximum stretching displacement was less than 0.0001 Å, and the maximum change in bending angles was below 0.001 rad. This criterion is sometimes too tight to be reached with density

TABLE II.
Performance of Geometry Optimization Using Skeletal Internal Coordinates

	Step 1		Final Step				
	Gradient (mdyn)			Gradient (mdyn)		Displ.	
Struct. No.	Norm	Max	*n*	Norm	Max	Max Stretches (Å)	Max Bendings (rad)
1	1.0616	0.4436	11	0.0008	0.0005	0.00012	0.00005
2a	1.1030	0.4958	13	0.0055	0.0030	0.00006	0.00024
2b	1.1026	0.4980	15	0.0064	0.0035	0.00005	0.00012
3	2.5071	2.2272	16	0.0018	0.0008	0.00014	0.00015
4a	1.7086	0.6337	11	0.0031	0.0017	0.00005	0.00002
4b	1.7084	0.6450	17	0.0090	0.0047	0.00018	0.00016
5	2.0526	0.9710	20	0.0095	0.0049	0.00008	0.00013
6a	0.3006	0.1256	12	0.0052	0.0024	0.00010	0.00021
6b	0.4086	0.3328	14	0.0033	0.0015	0.00013	0.00022
6c	0.9353	0.6899	15	0.0132	0.0050	0.00025	0.00300
6d	0.1921	0.1158	18	0.0200	0.0120	0.00031	0.00060
7a	0.4118	0.1770	13	0.0006	0.0003	0.00006	0.00006
7b	1.8839	1.7429	19	0.0037	0.0021	0.00024	0.00152
7c	0.3867	0.1890	16	0.0047	0.0037	0.00027	0.00137
7d	0.8725	0.7757	15	0.0039	0.0025	0.00033	0.00362
8a	0.8708	0.5411	8	0.0043	0.0013	0.00015	0.00002
8b	0.8509	0.5122	10	0.0087	0.0044	0.00022	0.00045
9	2.0927	0.8857	13	0.0026	0.0012	0.00014	0.00075
10a	1.6311	0.5953	11	0.0023	0.0008	0.00008	0.00004
10b	1.4159	0.6006	10	0.0036	0.0027	0.00005	0.00005
12	1.2920	0.8469	10	0.0004	0.0003	0.00003	0.00005
13	9.3092	4.8673	18	0.0045	0.0022	0.00040	0.00062
14	0.1396	0.0505	10	0.0069	0.0026	0.00025	0.00124

functional calculations, where numerical evaluation of integrals cannot be avoided. When the gradient and the energy started oscillating for numerical reasons, we stopped the geometry optimization. This situation with structures **6c** and **6d** was the most serious. However, the numerical uncertainty in the geometry is still an order of magnitude less that the absolute error of the method compared to experimental structures.

From Table II it is apparent that the performance of this optimization technique is in line with previous results of natural coordinate optimizations, especially if one takes the poor starting geometries into consideration. Also we used a simple diagonal Hessian, with force constants estimated from the force field of ferrocene, dibenzene-chromium, and $BzCr(CO)_3$.

An alternative representation of the skeletal degrees of freedom is possible with introducing metal–carbon bonds. The ligand stretching coordinates of $BzCr(CO)_3$ can be expressed as the equally weighted linear combination of all bonds between the metal and the bonded carbon atoms (s_i, $i = 1, \ldots, 6$) of the ligands: $q = s_1 + s_2 + s_3 + s_4 + s_5 + s_6$. Another linear combination, $q = 2s_1 + s_2 - s_3 - 2s_4 - s_5 + s_6$, can represent one of the tilting coordinates. The corresponding orthogonal tilting can be defined as $q = s_2 + s_3 - s_5 - s_6$. These internal coordinates were used before in empirical normal coordinate analysis of Bz_2Cr and $BzCr(CO)_3$.[13] We compared the performance of optimization using this alternative representation for $BzCr(CO)_3$, and the results are summarized in Table III. These results were obtained by replacing the skeletal stretching and the tilting coordinates by the appropriate linear combinations of metal–carbon bond stretchings, otherwise using natural coordinates including the skeletal internal coordinates defined above. In Table III we include the values of the skeletal stretching coordinates and that of a CC stretching coordinate along with the corresponding gradients in the first few and the last iterations. We note here that the replacement of the tilting coordinates should not make significant difference in the case of $BzCr(CO)_3$, since these coordinates are fixed by the molecular

TABLE III.
Performance of Geometry Optimization Using Centroid and Metal – Carbon Bond Representations

	Cr — Benzene Stretch			
	Centroid		Metal — C Bond	
Step	Coord.	Gradient	Coord.	Gradient
0	1.5822	−0.5411	5.1938	−0.2960
1	1.7626	0.1400	5.2925	−0.1080
2	1.7406	0.0377	5.3103	−0.1184
3	1.7288	0.0275	5.3331	−0.0871
4	1.7254	0.0243	5.3546	−0.0566
5	1.7158	0.0029	5.3989	−0.0274
8	1.7139	−0.0003		
Opt.	1.7139		5.590	
	C1 — C2 Stretch			
	Centroid		Metal — C Bond	
	Coord.	Gradient	Coord.	Gradient
0	1.4115	−0.0189	1.4115	0.0614
1	1.4142	0.0545	1.4027	−0.0333
2	1.4106	0.0380	1.4051	0.0031
3	1.4070	0.0094	1.4055	−0.0006
4	1.4064	0.0048	1.4053	−0.0051
5	1.4058	−0.0015	1.4060	0.0015
8	1.4057	−0.0003		
Opt.	1.4057		1.4057	
	Gradient Norm			
	Centroid		Metal — C Bond	
0		0.8708		0.7279
1		0.2861		0.2748
2		0.1487		0.1784
3		0.0622		0.1078
4		0.0463		0.0833
5		0.0215		0.0640
8		0.0042		

$BzCr(CO)_3$ staggered conformation.

symmetry. Therefore, the difference in performance of optimization is due to the different definition of the skeletal stretching coordinate.

It is clear from Table III that the centroid type coordinate remarkably improves the overall performance of optimization. The explanation for the different performance is due to the different coupling of the skeletal stretching coordinate with the CC stretches. To find an explanation for the coupling, one has to consider the derivatives of the skeletal stretching coordinates with respect to the displacement of the C atom in the plane of the ring. For the centroid-type coordinate this derivative is zero, while for the metal–carbon stretches this derivative is nonzero. To appreciate the magnitude of this coupling, one can look at the kinetic energy matrix elements corresponding to these coordinates, which are listed in Table IV, for $BzCr(CO)_3$. While the coupling G matrix element between CC stretch and skeletal coordinates are zero for the centroid representation, this is about 20% of the diagonal elements for the metal–carbon bond representation. This coupling explains the difference in the performance of the optimization between the two sets of coordinates. We also looked at the force constants in both representations; however, that did not show significant difference in the two representations.

Another qualitative explanation can be given by looking at the displacements that these internal

TABLE IV.
Comparison of G Matrix Elements in Centroid and Me — C Bond Representations.

	$BzCr(CO)_3$ Centroid	$BzCr(CO)_3$ Metal — C bond
CC stretch		
Diagonal	0.1667	0.1667
Skeletal stretch	0.0000	0.0248
Skeletal tilt	0.0000	−0.0254
Skeletal stretch, diagonal	0.0331	0.1355
Skeletal tilt, diagonal	0.0754	0.0850

Units are mdyn / Å, mdyn Å / rad, and mdyn / rad for stretches, stretch bend, and bends, respectively.

coordinates represent. All internal displacements have to leave the rest of the internal coordinates unchanged. For this reason, when the CC distance increases in the metal–carbon bond representation, the metal–ring distance has to decrease to keep the metal–carbon distance unchanged. This condition introduces large coupling between the skeletal stretch and the CC stretching coordinates.

To show the significance of natural internal coordinates for the optimization of transition metal complexes, we also compared it with optimization in Cartesian coordinates. The performance of Cartesian optimization largely depends on the quality of the Hessian used in the optimization. Therefore, to make it a fair comparison, we used a Hessian from a parametrized redundant force field in the Cartesian optimization. We used the parametrized Hessian supplied with release 2.01 of the ADF program. The performance of Cartesian optimization is compared to the natural coordinate optimization in Table V for five examples. The starting geometries and convergence criteria were the same for the two methods compared. In general, the natural internal coordinate optimization is about two to three times more efficient than the Cartesian optimization. One can also see from this comparison, that as the molecular symmetry is lowered the internal coordinate optimization is more and more advantageous. For highly symmetrical molecules many of the harmonic and anharmonic coupling constants are zero; therefore, the Cartesian optimization can also be fairly efficient. For metal complexes, besides the inherent deficiencies of the Cartesian optimization, the highly approximate parametrization of the Hessian and the poor starting geometries also contribute to the poor performance.

TABLE V.
Comparison of Performance Between Cartesian and Natural Internal Coordinate Optimizations.

Struct. No.	Natural Int. Coord. No. Cycles	Cartesian Coordinates Final Step		
		n	Gradient Max (mdyn)	Displ. Max (Å)
2a	13	52	0.0021	0.00082
3	16	50	0.0006	0.00101
7a	13	47	0.0005	0.00011
10a	11	18	0.0003	0.00011
13	18	61	0.0032	0.00081

Conclusions

In this paper we adopted the natural internal coordinate optimization of Forgarasi et al.[1] for applications to metal complexes with skeletal bonds. We suggested appropriate representations for the skeletal stretchings, bendings, tilts, and internal rotations of unsaturated organic ligands complexed to metals. We demonstrated how to construct internal coordinates using reference points defined by the geometrical center of bonded atoms. The application of these internal coordinates to geometry optimization showed that geometry optimization is very efficient using these coordinates in spite of the poor starting geometries and crude approximations of the Hessian. We also showed that the centroid approach is superior to the definition of skeletal motions with metal–carbon bonds. We also found that geometry optimization in natural internal coordinates is about two to three times more efficient than in Cartesian coordinates using a parametrized force field to approximate the Hessian.

Acknowledgments

Part of this work was done at the University of Calgary. I wish to thank my former supervisor Professor Tom Ziegler, the Academic Computing Services, and the Canadian Pacific Modelling Laboratory for providing computational resources. I would also like to thank my former colleagues Dr. John Lohrenz, Dr. Heiko Jacobsen, and Mr. Tom Woo for their encouragement to pursue this project and for continuing to apply this method in

their research. Financial support from the National Research Council is gratefully acknowledged. This article is issued as NRCC No. 39093.

References

1. (a) G. Forgarasi, X. Zhou, P. W. Taylor, and P. Pulay, *J. Am. Chem. Soc.*, **114**, 8191 (1992); (b) P. Pulay and G. Fogarasi, INTC program, University of Arkansas, Fayetteville, AK, 1990. This program automatically prepares the input for optimization in natural internal coordinates.
2. J. Baker, *J. Comput. Chem.*, **14**, 1085 (1993).
3. J. Pulay, G. Fogarasi, F. Pang, and J. E. Boggs, *J. Am. Chem. Soc.*, **101**, 2550 (1979).
4. (a) A. Bérces and T. Ziegler, *J. Phys. Chem.*, **98**, 13233 (1994); (b) A. Bérces, T. Ziegler, and L. Fan, *J. Phys. Chem.*, **98**, 1584 (1994).
5. (a) E. J. Baerends, D. E. Ellis, and P. Ros, *Chem. Phys.*, **2**, 41 (1973); (b) W. Ravenek, In *Algorithms and Applications on Vector and Parallel Computers*, H. J. J. te Riele, Th. J. Dekker, H. A. van de Vor, Eds., Elsevier, Amsterdam, 1987.
6. (a) P. M. Boerrigter, G. te Velde, and E. J. Baerends, *Int. J. Quantum Chem.*, **33**, 87 (1988); (b) G. te Velde and E. J. Baerends, *J. Comp. Phys.*, **99**, 84 (1992).
7. (a) S. H. Vosko, L. Wilk, and M. Nusair, *Can. J. Phys.*, **58**, 1200 (1980); (b) A. D. Becke, *Phys. Rev. A*, **38**, 2398 (1988); (c) J. P. Perdew, *Phys. Rev. B*, **33**, 8822 (1986), ibid., **34**, 7046 (1986).
8. (a) P. Császár and P. Pulay, *J. Mol. Struct.*, **114**, 31 (1984); (b) P. Pulay, *Chem. Phys. Lett.*, **73**, 393 (1980); (c) P. Pulay, *J. Comput. Chem.*, **3**, 556 (1982).
9. Programmed by A. G. Csaszar and P. G. Szalay, Eötvös University, Budapest, Hungary, 1984.
10. (a) S. Bhagavantam and T. Venkatarayudu, *Proc. Indian Acad. Sci.*, **9A**, 224 (1939); (b) *Theory of Groups and Its Application to Physical Problems*, Andhara University, Waltair, India 1951.
11. T. N. Doman, C. R. Landis, and B. Bosnich, *J. Am. Chem. Soc.*, **114**, 7264 (1992).
12. M. Kaupp and P. v. R. Schleyer, *J. Am. Chem. Soc.*, **114**, 8202 (1992).
13. (a) J. Brunvoll, S. J. Cyvin, and L. Schäfer, *J. Organomet. Chem.*, **27**, 69 (1971); (b) S. J. Cyvin, J. Brunvoll, and L. Schäfer, *J. Chem. Phys.*, **54**, 1517 (1971); (c) L. Schäfer, G. M. Begun, and S. J. Cyvin, *Spectochim. Acta*, **28A**, 803 (1972).